Supplementary Information

A flexible, multi-layered protein scaffold maintains the slit in between glomerular podocytes

Grahammer F, Wigge C, Schell C, Kretz O, Patrakka J, Schneider S, Klose M, Arnold SJ, Habermann A, Bräuniger R, Rinschen MM, Völker L, Bregenzer A, Rubbenstroth D, Boerries M, Kerjaschki D, Miner JH, Walz G; Benzing T, Fornoni A, Frangakis AS and Huber TB

Supplementary Figure legends

Supplementary Figure 1: Expression profile of NEPHRIN and NEPH1.

(**A,B**) Expression of *Nphs1* in the cerebellum anlage is dependent on time and vanishes by E15,5. (**C,D**) Kidney and pancreas are the only other sites of embryonic (E13,5) expression of *Nphs1*. (**E-H**) *Neph1* in contrast shows a widespread expression in the CNS, lung, kidney and gut. In newborn mice NEPHRIN on the protein level can only be detected in kidney and pancreas, but not in brain. (**I**) By contrast, NEPH1 can be readily detected in kidney, brain, heart, lung, liver, pancreas, gut and skeletal muscle. (**J,K**) Proof of constitutive *Nphs1* knock-out by the absence of NEPHRIN protein. (**L,M**) Proof of constitutive *Neph1* knock-out by the absence of NEPH1 protein .

Supplementary Figure 2: Expression profile of *Neph2* and *Neph3*.

(**A + insert**) At E13.5 *Neph2* expression is widespread in central and peripheral nervous tissue, but absent in kidney. (**B + insert**) At the same stage of embryonic

development *Neph3* expression is restricted to forebrain, cerebellum anlage, pancreas and is lacking in kidney as well. (**C**,**D**) Immuno precipitation of brain lysates was used to confirm knock-out of NEPH2 and NEPH3 using the targeting strategies out-lined in Fig. 1 G,H. (**E**) RT-PCR of isolated mouse podocytes and mouse brain of *Nphs1, Neph1, Neph2* and *Neph3*. *Nphs1*, *Neph1* and *Neph3* can be detected in isolated mouse podocytes of 8 week old animals while *Neph2* mRNA is absent. (**F**) On a protein level also NEPH3 is absent in isolated mouse glomeruli, while it can be detected faintly in mouse brain.

Supplementary Figure 3: Residual slit diaphragms in mouse and human *Nphs1* deletion show altered slit width and distance to the GBM. (**A,D**) Murine *Nphs1* deletion leads to narrower and more apically located remnant SDs (17% open SDs, width: n=32 from 3 *Nphs1 -/-* animals vs n=312 from 3 wild-type animals; distance to GBM: n=13 from 3 *Nphs1* -/- animals vs. n=94 from 3 wild-type animals; Student's t-test). (**B, E**) In mice with *Neph1* deletion, slit width was only very slightly reduced compared with wild-type animals while distance to the GBM was significantly increased (30% open SDs, width: n=188 from 3 *Neph1 -/-* animals vs n=243 from 3 wild-type animals; distance to GBM: n=120 from 3 *Neph1* -/- animals vs. n=98 from 3 wild-type animals; Student's t-test). (**C,F**) Similarly, in human patients with *Fin major* mutations remnant SDs were narrow and located in apical distance to the GBM (width: n=77 from 3 *Fin major* patients; distance to GBM n=46 from 3 *Fin major* patients).

Supplementary Figure 4: Residual slit diaphragms in human pathology specimen with congenital nephrotic syndrome. (**A**-**D**) In approximately 5-10% of SDs, residual slit diaphragms are still apparent in both fetal and infant tissue from

53 patients carrying *Fin major* mutations in *NPHS1*. Example of a kidney specimen of a
54 *Fin major/major* fetus (*NPHS1* -/- without residual function) showing residual SD like
55 cell-cell contacts (yellow arrows in overview **A**, **C** and details **B**, **D**). (**E**, **F**) In a
56 nephrectomy specimen (**E**) of another *Fin major/major* patient at the age of 2 years
57 we were able to indeed demonstrate NEPH1 immunoreactivity (**F** yellow arrows)
58 using Immuno–EM.
59
60 **Supplementary Figure 5: *Neph2*$^{-/-}$ and *Neph3*$^{-/-}$ mice do not exhibit any overt**
61 **phenotype.** (**A-F**) Compared with *control (***A**, **D***)* animals *Neph2*$^{-/-}$ (**B**, **E**) and *Neph3*$^{-/-}$
62 (**C**, **F**) animals show normal light microscopic and TEM appearance. (**G**, **H**) Neither
63 *Neph2*$^{-/-}$ (**G**) nor *Neph3*$^{-/-}$ (**H**) 6 month old adult constitutive animals (black columns)
64 do display any proteinuria compared with wild type animals (white columns; at least 6
65 - *Neph2*$^{-/-}$ or 8 – *Neph3*$^{-/-}$ animals per group were tested).
66
67 **Supplementary Figure 6: NEPHRIN is absent from chicken glomerula. (A-F**)
68 NEPHRIN cannot be detected by immunofluorescence in chicken glomerula (**A** –
69 ZO1 green ,**B** – NPHS1 red, **C** - MERGE, blue Hoe 33342) whereas NEPH1 can be
70 easily and specifically detected in chicken podocytes (**D** – ZO1 green, **E** – NEPH1
71 red, **F** – MERGE, blue Hoe 33342). (**G-I**) The same holds true for PODOCIN and ZO-
72 1 which can both be detected in podocytes within the chicken glomerulum (**G** – ZO1
73 green, **H** – PODOCIN red, **I** - MERGE, blue Hoe 33342). (**J**-**L**) WT-1, one of the main
74 transcription factors active in mammalian podocytes, is also expressed in chicken (**J** -
75 ZO-1 green, **K** - WT-1 red, **I** - MERGE, blue Hoe 33342).
76
77

78 # Methods

79

80 **Animals**

81 All animal experiments were conducted according to the NIH Guide for the care and
82 use of Laboratory animals as well as in accordance with the German law for the
83 welfare of animals, and were approved by local authorities (Regierungspräsidium
84 Freiburg G-09/23, G-10/100, X12/06J and X13/04J). Mice were housed in a SPF
85 facility with free access to chow and water and a 12 h day/night cycle. Breeding and
86 genotyping were done according to standard procedures. Urinary albumin and
87 creatinine were measured using a fluorimetric albumin test kit (Progen, PR2005,
88 Heidelberg, Germany) or enzymatic colorimetric creatinine kit (LT-SYS, Lehmann,
89 Berlin, Germany) following the manufacturers' instructions.

90

91 We generated a *Nphs1* floxed mouse with loxP sites flanking exons 1B-5 using
92 commercial support by Ozgene (Bentley, WA, Australia). The targeting vector
93 included three loxP sites, one in the 5'-UTR of exon 1B, one in the 5'-UTR of Exon
94 1A and the third flanking the PGK-neo selection cassette downstream of exon 5. The
95 complete targeting vector was then screened by sequencing and restriction enzyme
96 digestions. *Neph1* animals were generated by Genoway (Lyon, France) targeting
97 Exons 12-15 of mouse *Neph1* in a 9.7 kB mouse genomic DNA fragment in a
98 C57Bl/6 BAC clone, which was recombinated into 129Sv/Pas ES cells.
99 Recombination was confirmed using PCR and Southern blot. Male floxed mice for
100 *Nphs1* and *Neph1* were crossed with female *Sox2Cre* deleter mice to obtain
101 heterozygous constitutive knockout mice(1). Null mice were obtained by
102 heterozygous breeding and genotyping was performed using standard procedures.
103 We generated conditional knockout mice of the *Neph2* and *Neph3* loci by

104 homologous recombination in 129 Sv/J (129S7/SvEvBrd) embryonic stem cells.
105 Briefly, exon 2 of the endogenous *Neph2* locus was replaced by a cDNA consisting of
106 exon 2-16 flanked by loxP sites that was followed by an internal ribosomal entry site
107 (IRES) to enable expression of beta-galactosidase from the bacterial lacZ gene. The
108 *Neph3* locus was targeted by inserting loxP sites into exon 1 upstream of the start
109 codon and into the intronic sequence between exon 2 and exon 3. Cre-mediated
110 recombination excises parts of the 5'-UTR and the coding sequence, including the
111 regions encoding the start codon and the signal peptide, of the *Neph3*-transcript.
112 Gt(ROSA)$^{26Sortm4(ACTB-tdTomato,-EGFP)Luo/J}$ mice were purchased from JaxLab (Bar
113 Harbour, Massachusetts, USA) (2) , *hNPHS2*Cre mice were a generous gift of MJ
114 Möller (University of Aachen, Department of Nephrology, Aachen, Germany).
115
116 **Human archive material**
117 The use of human kidney samples was accepted by the local ethical committee
118 (Hospital for Children and Adolescents, Helsinki, Finland). One sample was derived
119 from an aborted fetus and the other was a nephrectomy specimen obtained from a 2
120 year old boy. Both patients carried a two base pair deletion after nucleotide 121
121 (nt121delCT), resulting in a stop codon shortly after the signal peptide of *NPHS1*
122 leading to a *Fin major* phenotype.
123
124 **Morphological analysis**
125 Kidneys were perfusion fixed in 4% phosphate buffered paraformaldehyde,
126 embedded in paraffin and further processed for PAS (Periodic Acid–Schiff) staining.
127 For ultrastructural analysis kidneys were also fixed in 4% phosphate buffered
128 paraformaldehyde. Samples were postfixed in 1% osmium tetroxide in the same
129 buffer for 1 h and stained *en bloc* in 1% uranyl acetate in 10% ethanol for 1 h,

130 dehydrated in ethanol, and embedded in LX112 (Fisher-Scientific, Schwerte,
131 Germany). Semithin sections were stained with toluidine blue. Thin sections were
132 stained with uranyl acetate and lead citrate and examined in a Jeol JEM 1200EX
133 electron microscope (JEOL, Eching, Germany). For SEM mouse and chicken kidneys
134 were perfused through the renal artery with phosphate-buffered saline (PBS, 0.9%
135 NaCl in 10mM phosphate buffer, pH7.4) followed by paraformaldehyde (4%) lysine
136 (75mM) periodate (10mM) fixative in 0.15M sucrose, 37.5mM sodium phosphate
137 (modified PLP) and post-fixed overnight at 4°C in the same fixative. 200µm thick
138 vibratome sections were cut and dehydrated in a series of graded ethanol solutions.
139 Ethanol and baskets containing vibratome sections were placed in a critical point
140 drying apparatus (Baltec, Wetlar, Germany), the samples were purged with cold
141 liquid CO2 at elevated pressure, and then brought to supercritical pressure and
142 temperature for incubation and equilibration. Then the pressure was slowly reduced,
143 while maintaining supercritical temperatures. After the bleeding process was
144 completed, dried samples were mounted onto placeholders with sticky pads, sputter-
145 coated with gold and examined using a scanning electron microscope (FEI, Hillsboro,
146 OR, USA).
147
148 **Western blot and immunofluorescence**
149 Tissues were glass-glass-homogenized in lysis buffer (containing either 20mM
150 CHAPS and 1% Triton X-100 [WB shown in Suppl. Figure 1] or RIPA Buffer
151 containing: 50mM Tris/HCl pH 7,5, 1 mM EGTA, 1 mM EDTA, 1% (w/v) Triton X-100,
152 0,1 % (w/v) SDS, 50 mM NaF, 150 mM NaCl, 0,5% (w/v) Na-Deoxycholate, 0,1
153 %(v/v) 2-mercaptoethanol, 1mM Na-Orthovanadate, Roche Ultra complete
154 proteinase inhibitor cocktail and Roche Phospho-STOPP as indicated by the
155 manufacturer (Roche, Mannheim ,Germany) and ddH_2O ad final volume; 15µl lysis

156 buffer per 1 mg of tissue were used [WB shown in Suppl. Figure 2]). After
157 centrifugation (1000xg, 5min, 4 °C), the supernatant was recovered and the protein
158 concentration was determined by DC Protein-Assay (Bio-Rad, Munich, Germany).
159 Samples were heated after addition of 2x Laemmli buffer (inlcuding 100 mM DTT) at
160 42°C for 30 min. Equal amounts of protein (80µg per lane) were separated on SDS
161 page. HRP coupled 2nd antibodies and ECL in combination with a conventional x-ray
162 system (films: Fuji, Tokio, Japan; developer: AGFA, Mortsel, Belgium) were used to
163 detect western blot bands. For immunofluorescence kidneys were frozen in OCT
164 compound and sectioned at 5µm (Leica Kryostat, Wetzlar, Germany). The sections
165 were fixed with 4% paraformaldehyde in phosphate buffered saline (PBS), blocked in
166 PBS containing 5% BSA + 5% Normal Donkey Serum (Jackson Immuno Research,
167 Suffolk, UK) and incubated for 45 min with primary antibodies as indicated. After
168 several PBS rinses, fluorophore-conjugated secondary antibodies (Life Technologies,
169 Darmstadt, Germany) were applied for 30 min. Images were taken using a Zeiss
170 fluorescence microscope equipped with a 20x and 63x water immersion objective
171 (Zeiss, Oberkochen, Germany).
172
173 **Antibodies**
174 We generated a NEPH1 peptide-antibody against mNEPH1 aa 767-788 by
175 immunizing a rabbit with the corresponding peptide coupled to Keyhole Limpet
176 Hemocyanin using Freud's complete adjuvant on d1 and Freund's incomplete
177 adjuvant on d20, d30 and d40. From d61 a boost was given every 15 days. The final
178 bleed was performed on d130 after a positive immunoreactive testbleed on d120,
179 and the serum was affinity purified against the immunogenic peptide used (Pineda
180 Antikörper, Berlin, Germany). The following other antibodies were used: guinea pig
181 anti-NEPHRIN (gp-NP2; Progen, Heidelberg, Germany), mouse anti-ZO1 (33-9100;

182 Life Technologies, Karlsruhe, Germany), sheep anti-NEPH2 (AF 4910; R&D,
183 Wiesbaden, Germany) , goat anti-NEPH3 (AF 2930; R&D, Wiesbaden, Germany)
184 rabbit anti-CD2AP (generous gift of A. Shaw, Washington University, St. Louis, MO,
185 USA) (3), rabbit anti-WT1 (sc 192; Santa Cruz, CA, USA), rabbit anti-NPHS2 (P0372;
186 Sigma, Schnelldorf, Germany), rat anti-NIDOGEN (MAB1946; Merck Millipore,
187 Schwalbach, Germany), rabbit anti-TRPC6 (generous gift of V. Flockerzi, University
188 Homburg, Homburg, Germany) (4).
189
190 **In situ hybridization**
191 Mouse kidney postnatal day 1 RNA served to clone fragments of coding and 3′-UTR
192 of mouse *Neph1* using One-Step PCR Kit (Qiagen, Heidenheim, Germany). PCR
193 fragments were inserted into *pBluescript (SK*+) vector (Invitrogen, Carlsbad, CA)
194 using *SpeI* and *XhoI* restriction sites. For mouse *Nephrin*, *Neph2* and *Neph3* mouse
195 kidney postnatal day 1 RNA served to clone PCR fragments using One-Step PCR Kit
196 (Qiagen). PCR fragments were inserted into *pBluescript (KS-)* vector (Invitrogen,
197 Carlsbad, CA) using *NotI* and *MluI* restriction sites. *pBluescript* Vector was linearized
198 and digoxigenin-(DIG)-labeled antisense riboprobes were generated using T7-RNA-
199 polymerase (Roche, Mannheim, Germany); for Neph1, T3 was used (Roche). For
200 paraffin section ISH, slides were progressively rehydrated and permeabilized with
201 proteinase K for 5 min. After prehybridization (20 min), hybridization with DIG-UTP
202 probes took place overnight in standard saline citrate (SSC; pH 4.5; containing 50%
203 formamide) at 68 °C. Specimens were then incubated with alkaline phosphatase-
204 conjugated anti-DIG Fab fragments (Roche, Mannheim, Germany) at a dilution of
205 1:3000 for 2 h at room temperature. Alkaline phosphatase was detected using
206 chromogenic conversion of BM Purple (Roche). Slides were then progressively
207 dehydrated in xylol, and mounted. The following primers were used:

208 *Nphs1*

209 5’-cgcgggacgcgtGTGGTCTTCTGTTGCTTTCCAATG-3’,

210 5’-cgcggggcggccgcTCTGGTCTTCTCCAAGGCTGTAGG-3´

211 *Neph1*

212 [Neph1F1] 61-82 5'- AAACTAGTTGCTGTATGCTGACTACCGTGC -3'

213 [Neph1B1] 633-612 5'- AACTCGAGTGGGATGTTACTGGGAGACCTG -3';

214 *Neph2*

215 fpISHneph2m 5'-CGCGGGACGCGTTAACTGCACACCCAAGTTGC-3'

216 rpISHneph2m 5'-CGCGGGGCGGCCGCTGCTCTCCTGAGAGGTGGTT-3'

217 *Neph3*

218 fpISHneph3m 5'-CGCGGGACGCGTGAAGTTGGAGGGGAACCAGT-3'

219 rpISHneph3m 5'-CGCGGGGCGGCCGCACCACCCTGGAAGGTCTCTT-3’

220

221

222 **Isolation of Mouse Glomeruli and Podocytes**

223 We essentially used the same method as described previously (5). Briefly, kidneys
224 were dissected together with the abdominal aorta and transferred into dishes filled
225 with 37°C prewarmed Hank’s buffered salt solution (HBSS). Each kidney was
226 perfused slowly through the renal artery with 4 ml 37°C warm bead solution and 1 ml
227 bead solution plus enzymatic digestion buffer [containing: collagenase 300 U/ml
228 (Worthington, Collagenase Type II, USA), 1 mg/ml pronase E (Sigma P6911,
229 Germany) DNase I 50 U/ml (Applichem A3778, Germany)]. Kidneys were minced
230 into 1 mm^3 pieces using a scalpel. After addition of 3 ml digestion buffer they were
231 incubated at 37°C for 15 min on a rotator (100rpm). The solution was pipetted up and
232 down with a cut 1000µl pipette tip every 5 min. After incubation all steps were
233 performed at 4 °C or on ice. The digested kidneys were gently pressed twice through

234 a 100 µm cellstrainer and the flow through was washed extensively with HBSS. After
235 spinning down, the supernatant was discarded and the pellet resuspended in 2 ml
236 HBSS. These tubes were inserted into a magnetic particle concentrator and the
237 separated glomeruli were washed twice. Glomeruli were resuspended in 2 ml
238 digestion buffer and incubated for 40 min at 37°C on a thermomixer shaking at
239 1400/min. During this incubation period the glomeruli were sheared with a 27G
240 needle at 15 min, and mixed by pipetting twice at 5, 10, 15, 20 and 25 min using a
241 glass pipette. Podocytes were loosened at 10, 20, 30 min by vortexing once. After 40
242 min the solution was vortexed three times and the digestion result controlled by
243 fluorescence microscopy. Samples were put on a magnetic particle concentrator
244 again to eliminate beads and glomerular structures void of podocytes. The
245 supernatant was pooled and the magnetic particles discarded. The cell suspension (2
246 ml) was sieved through a 40 µm pore size filter on top of a 50 ml Falcon tube, rinsed
247 with 10 ml of HBSS. Cells were collected by centrifugation at 1500 rpm for 5 min at
248 4°C, resuspended in 0.5 ml of HBSS supplemented with 0.1% BSA plus DAPI
249 (1µg/ml). To separate GFP-expressing (GFP+) and GFP-negative (GFP-) cells,
250 glomerular cells were sorted with a Mo-Flo cell sorter (Beckman Coulter) with a Laser
251 excitation at 488nm (Power 200 mW) and a sheath pressure of 60 PSI. Cells were
252 kept at 4°C before entering the FACS machine and thereafter, while temperature
253 during the sorting procedure (approx. 3 min) was 22°C. Only viable (DAPI negative)
254 cells were sorted (laser excitation 380nm, power 80 mW).
255
256 **RT PCR of *Neph1, Neph2, Neph3* and *Nphs1***
257 Under RNase-free conditions RNA was extracted from mouse brain and isolated
258 mouse podocytes with the chloroform/phenol method and DNase digested at the end
259 of the preparation process. The RT reaction was performed using dNTPs (Promega,

260 Mannheim, Germany), random primers (Invitrogen, Karlsruhe, Germany), MMLV
261 Reverse Transcriptase (Promega, Mannheim, Germany) and RNAse out (Invitrogen,
262 Karlsruhe, Germany) following the instructions of the manufacturers. 40ng of RNA
263 was used for each reaction. RT-PCR was done using the Taq DNA Polymerase Kit
264 from Invitrogen (Karlsruhe, Germany). The following primers were used:
265 *mNeph1s* CTGCCACCATCATTTGGTTC
266 *mNeph1as* GTGCTGACATTGGTGCTCCC
267
268 *mNeph2s* GATGCTGTCTTCAGCTGTGCGT
269 *mNeph2as* CCCAGCATCCTCTTGGCGGAC
270
271 *mNeph3s* CCGCAACCGGCTAGGAGAGGGA
272 *mNeph3as* GCTGCACCAGCCACAATCCG
273
274 *mNphs1s* GGACTGGTTCGTCTTGTCGT
275 *mNphs1as* TCAAAGCCAGGTTTCCACTC
276
277 Resulting products were visualized using a 2% Agarose Gel and sequenced to prove
278 specificity.
279
280 **Structural modeling of NEPHRIN and NEPH1**
281 For mouse NEPHRIN databases (uniprot Q9QZS7, NCBI: NP_062332.2) predict 8 N-
282 terminal immunoglobulin type C2 domains and one C-terminal fibronectin type III
283 domain. A tenth Ig domain (between Ig6 and Ig7, aa650-753) was predicted here
284 with sequence alignments of all mouse NEPHRIN Ig domains and with the use of
285 PHYRE2 (6).

286 For all 10 separate domains of mouse NEPHRIN and 3 domains of mouse NEPH1
287 (uniprot Q80W68, ncbi: NM_019459.2) PHYRE2 was used to obtain optimal
288 templates. The following PDB structures were used to generate a model from the N-
289 to C-terminus of mouse NEPHRIN: 2yuv, 1vca, 2eo9, 1mfb, 2wwm, 1lc1, 2wwm,
290 2v5m, 1ie5, 2ed8 and Neph1: 3b43 (Ig3-4), 2cry (Ig5). For NEPH1 the Ig domains 1
291 and 2 of the mouse crystal structure were used (pdb: 4ofd).
292 Using the Swiss pdb-viewer missing loops were closed, single domains were
293 connected and aligned in a linear order to obtain the longest possible protein
294 structure. The arrangement of the Ig domains in the crystal structure of NEPH1 was
295 not changed but two missing loops were generated. Also the c-terminal unfolded
296 region was maximally spread and linked with a transmembran a-helix generated by
297 the Swiss pdb-viewer. Both intracellular domains were omitted. The structures were
298 visualized using PyMOL.
299
300 **Electron tomography**
301 For electron tomography (ET), kidney tissue was prepared as described above. Thick
302 sections (300nm) were cut from Epon blocks using an EM UC7 ultramicrotome (Leica
303 AG, Wetzlar, Germany) and transferred onto formvar-coated copper slot grids. 10nm
304 colloidal gold particles (CMC, Utrecht, The Netherlands) were applied to the sections
305 as fiducial markers. Samples were analyzed using a Tecnai F30 transmission
306 electron microscope (FEI, Eindhoven, The Netherlands) operated at 300 kV. Tilt
307 series were acquired between -60° and +60° using an increment of 1° and a
308 magnification of 9400x on a US 4000 CCD camera (Gatan Inc., Pleasanton, CA,
309 USA). Afterwards tilt series were aligned and reconstructed using IMOD software (7).
310 For visualization of the filtration barrier, Amira software (FEI, Eindhoven, The
311 Netherlands) was used.

312 **Cryosectioning and cryo electron tomography**

313 Isolated kidneys of *mT/mG*hNphs2Cre* mice(8) were first perfused with 1ml of 20%
314 Dextran in PBS followed by a second perfusion with 1ml 25% Dextran containing
315 10nm Protein-A-Gold (CMC, Utrecht, The Netherlands). The tissue was cut into small
316 pieces and placed in gold-plated copper carriers type 662 with 0.2µm recess
317 (Wohlwend, Sennwald, Switzerland) filled with 20% Dextran. Carriers were closed
318 with flat gold-plated type 663 carriers (Wohlwend) coated with Lecithin prior to high-
319 pressure freezing with HPM-010 (Abra, Abrafluid AG, Widnau, Switzerland). Carriers
320 were observed in a Linkam Cryostage on a Zeiss LSM 700 Confocal Microscope
321 (Zeiss, Oberkochen, Germany) to identify fluorescent glomeruli. Distances of
322 glomeruli to tissue edges and/or carrier edges were measured. Based on those
323 measurements glomeruli were target trimmed and cryosectioned in an Ultracut FC6
324 (Leica, Wetzlar, Germany). Sections were transferred to C-flat CF 2/1 Grids and
325 attached with a Haug Charging System (Haug, Leinfelden-Echterdingen, Germany).
326 Grids were mounted in FEI autogrids and analyzed in a Titan Krios TEM (FEI
327 company, Eindhoven, The Netherlands) operated at 300kV. Tomography tilt series
328 between (-60C° to +60C°) were acquired using a nominal defocus of -5µm and a total
329 dose < 60 $e^-/Å^2$ on a US 4000 CCD camera (Gatan Inc, Pleasanton, CA, USA).

330

331 **Statistics**

332 Data are expressed as mean ± SEM. Statistical comparisons were performed using
333 the GraphPad Prism Software Package 6.02 (GraphPad Software, La Jolla, CA.
334 USA) with two-tailed Student's t-test, Wilcoxon test or ANOVA including respective
335 corrections where indicated. Differences with p values below 0.05 were considered
336 significant.

337

338 **Supplementary Information References**

339 1. Hayashi, S., Tenzen, T., and McMahon, A.P. 2003. Maternal inheritance of
340 Cre activity in a Sox2Cre deleter strain. *Genesis* 37:51-53.
341 2. Muzumdar, M.D., Tasic, B., Miyamichi, K., Li, L., and Luo, L. 2007. A global
342 double-fluorescent Cre reporter mouse. *Genesis* 45:593-605.
343 3. Dustin, M.L., Olszowy, M.W., Holdorf, A.D., Li, J., Bromley, S., Desai, N.,
344 Widder, P., Rosenberger, F., van der Merwe, P.A., Allen, P.M., et al. 1998. A
345 novel adaptor protein orchestrates receptor patterning and cytoskeletal polarity
346 in T-cell contacts. *Cell* 94:667-677.
347 4. Tsvilovskyy, V.V., Zholos, A.V., Aberle, T., Philipp, S.E., Dietrich, A., Zhu,
348 M.X., Birnbaumer, L., Freichel, M., and Flockerzi, V. 2009. Deletion of TRPC4
349 and TRPC6 in mice impairs smooth muscle contraction and intestinal motility
350 in vivo. *Gastroenterology* 137:1415-1424.
351 5. Boerries, M., Grahammer, F., Eiselein, S., Buck, M., Meyer, C., Goedel, M.,
352 Bechtel, W., Zschiedrich, S., Pfeifer, D., Laloe, D., et al. 2013. Molecular
353 fingerprinting of the podocyte reveals novel gene and protein regulatory
354 networks. *Kidney International* 83:1052-1064.
355 6. Kelley, L.A., and Sternberg, M.J. 2009. Protein structure prediction on the
356 Web: a case study using the Phyre server. *Nature Protocol* 4:363-371.
357 7. Kremer, J.R., Mastronarde, D.N., and McIntosh, J.R. 1996. Computer
358 visualization of three-dimensional image data using IMOD. *Journal Structural*
359 *Biology* 116:71-76.
360 8. Wanner, N., Hartleben, B., Herbach, N., Goedel, M., Stickel, N., Zeiser, R.,
361 Walz, G., Moeller, M.J., Grahammer, F., and Huber, T.B. 2014. Unraveling the
362 role of podocyte turnover in glomerular aging and injury. *J Am Soc Nephrol*
363 25:707-716.

364

365

Supplemental Table I

Domain	**Protein**	**PDB-code**	**sequence identity (%)**	**sequence similarity (%)**
NEPHRIN				
Ig1	2nd Immunoglobulin Domain of Slow Type Myosin-Binding Protein C	2yuv	25,3	49,4
Ig2	VCAM-1	1vca	20,4	38,7
Ig3	fifth ig-like domain from human Roundabout homo1	2eo9	26,2	46,4
Ig4	IGG1-LAMBDA SE155-4 FAB (LIGHT CHAIN)	1mfb	22,8	43
Ig5	Obscurin like Protein	2wwm	18,8	46,3
Ig6	Icam-1	1lc1	21,6	40,9
inter Ig6-7	Obscurin like Protein	2wwm	27	44,6
Ig7	Dscam	2v5m	23,6	41,7
Ig8	NCAM Ig3	1ie5	30,6	48,2
Fibronectin	Netrin Rezeptor	2ed8	29,5	47,7
NEPH1				
Ig1	Neph1	4ofd	95,5	95,5
Ig2	Neph1	4ofd	95,5	95,5
Ig3	Titin	3b43	21,4	39,9
Ig4	Titin	3b43	21,4	39,9
Ig5	Kirrel3	2cry	63,8	77,7

Summary of the respective templates used for modelling each individual Ig fold in NEPHRIN and NEPH1, respectively.

Supplemental Figure 1

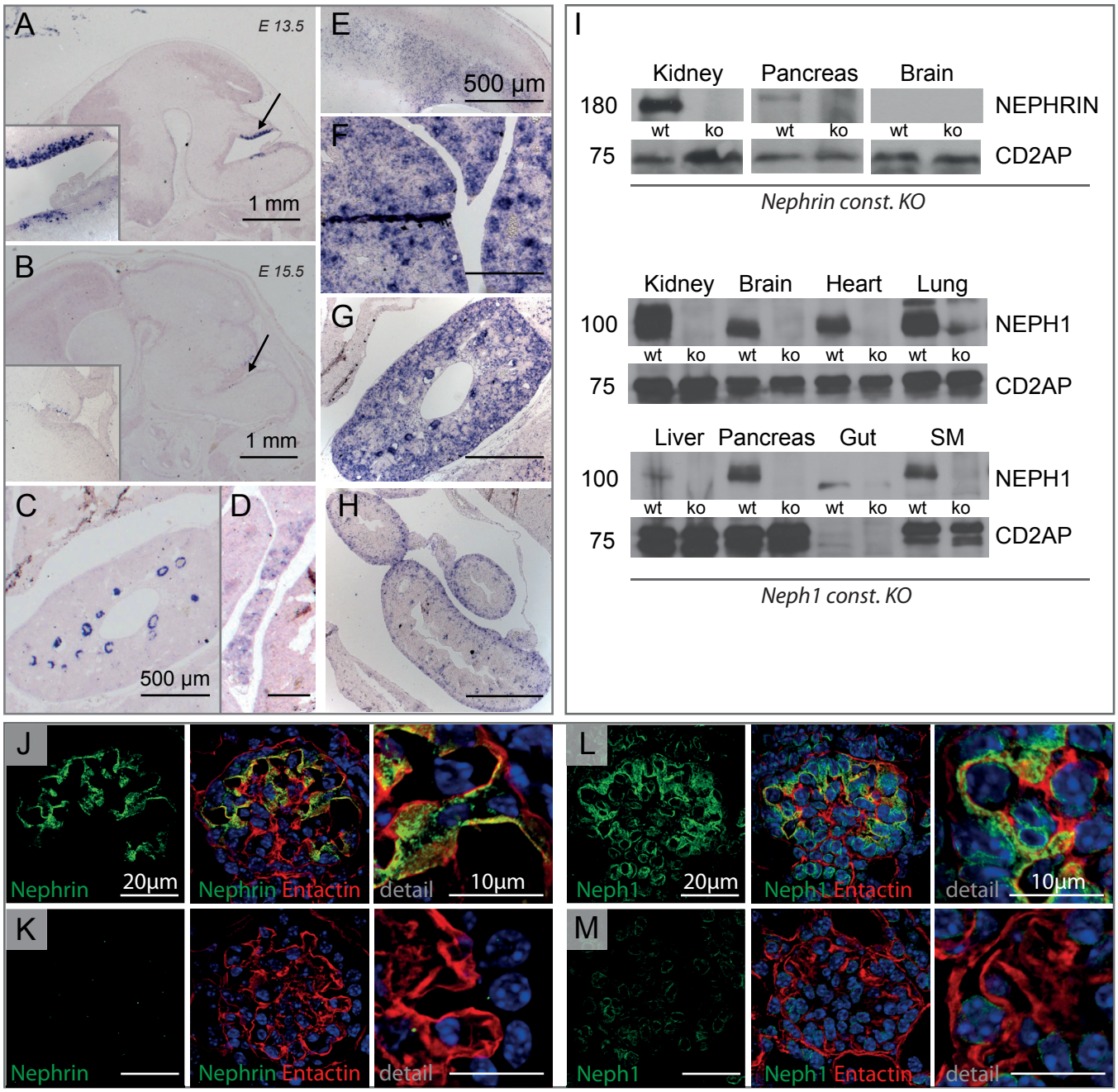

Supplemental Figure 2

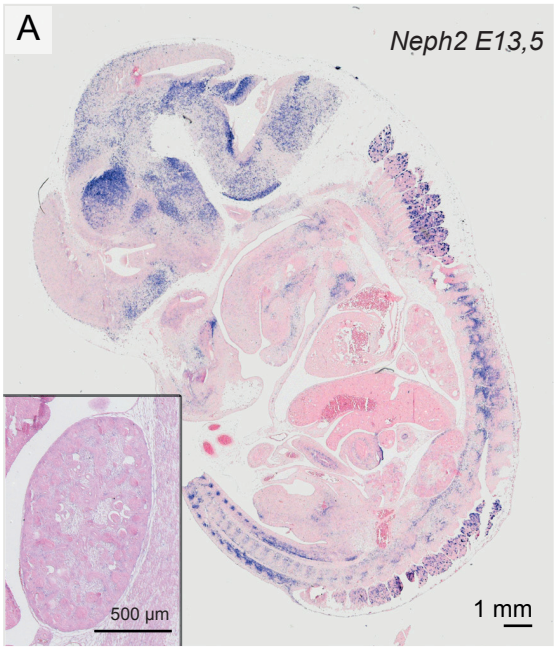

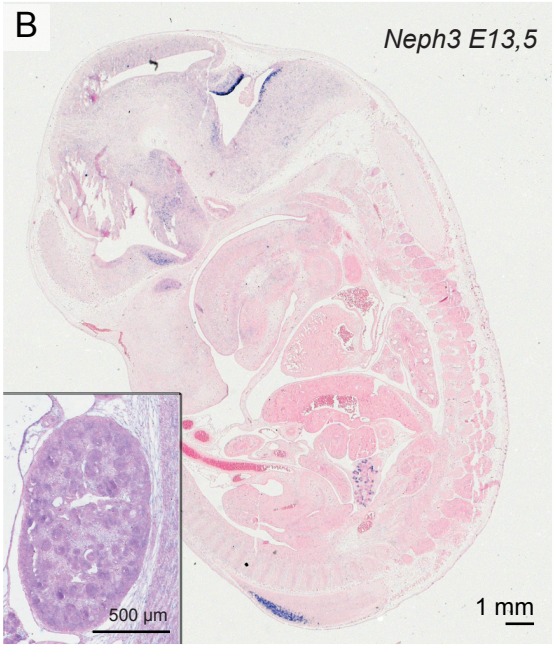

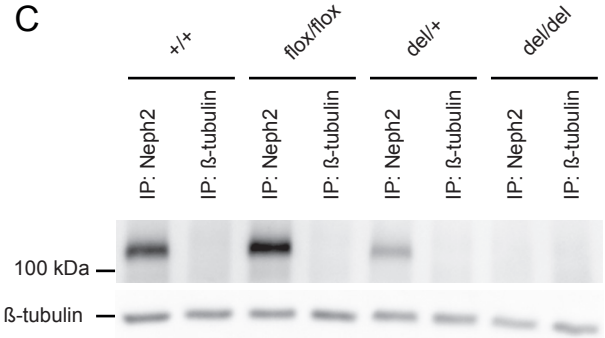

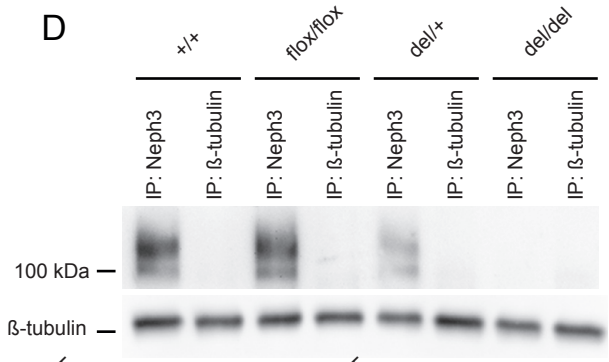

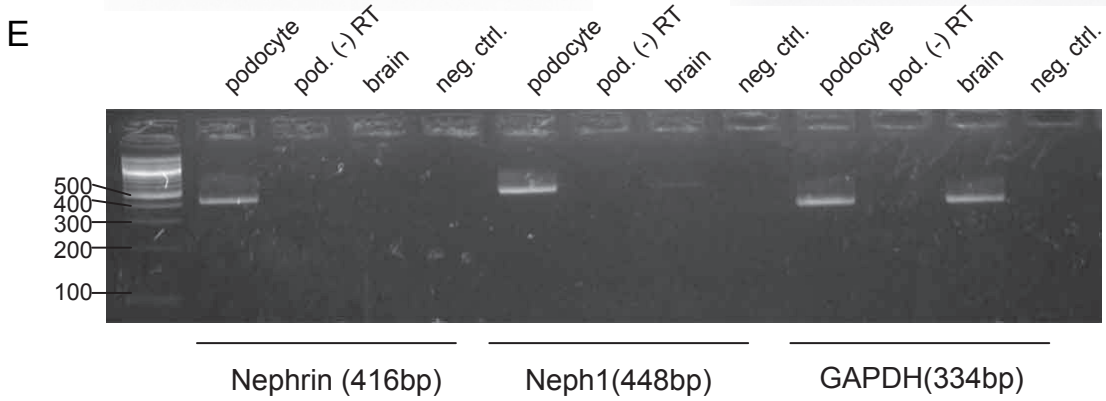

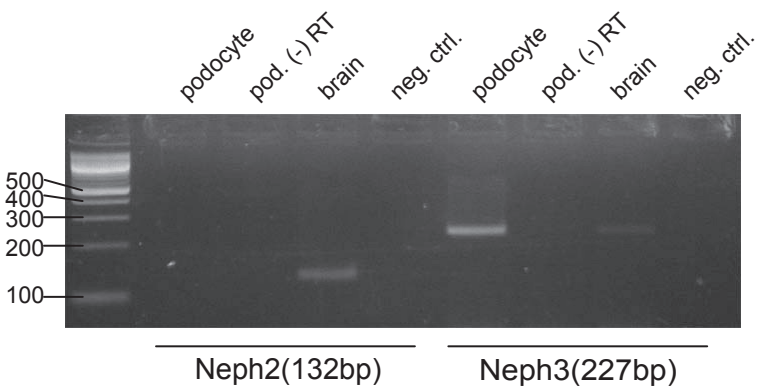

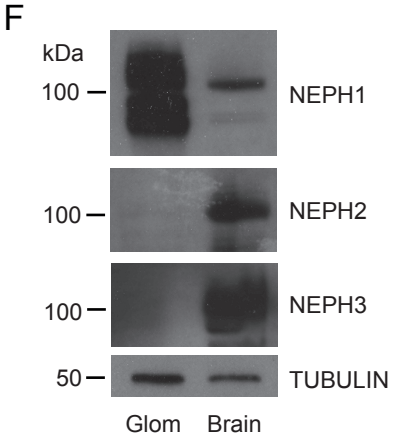

Supplemental Figure 3

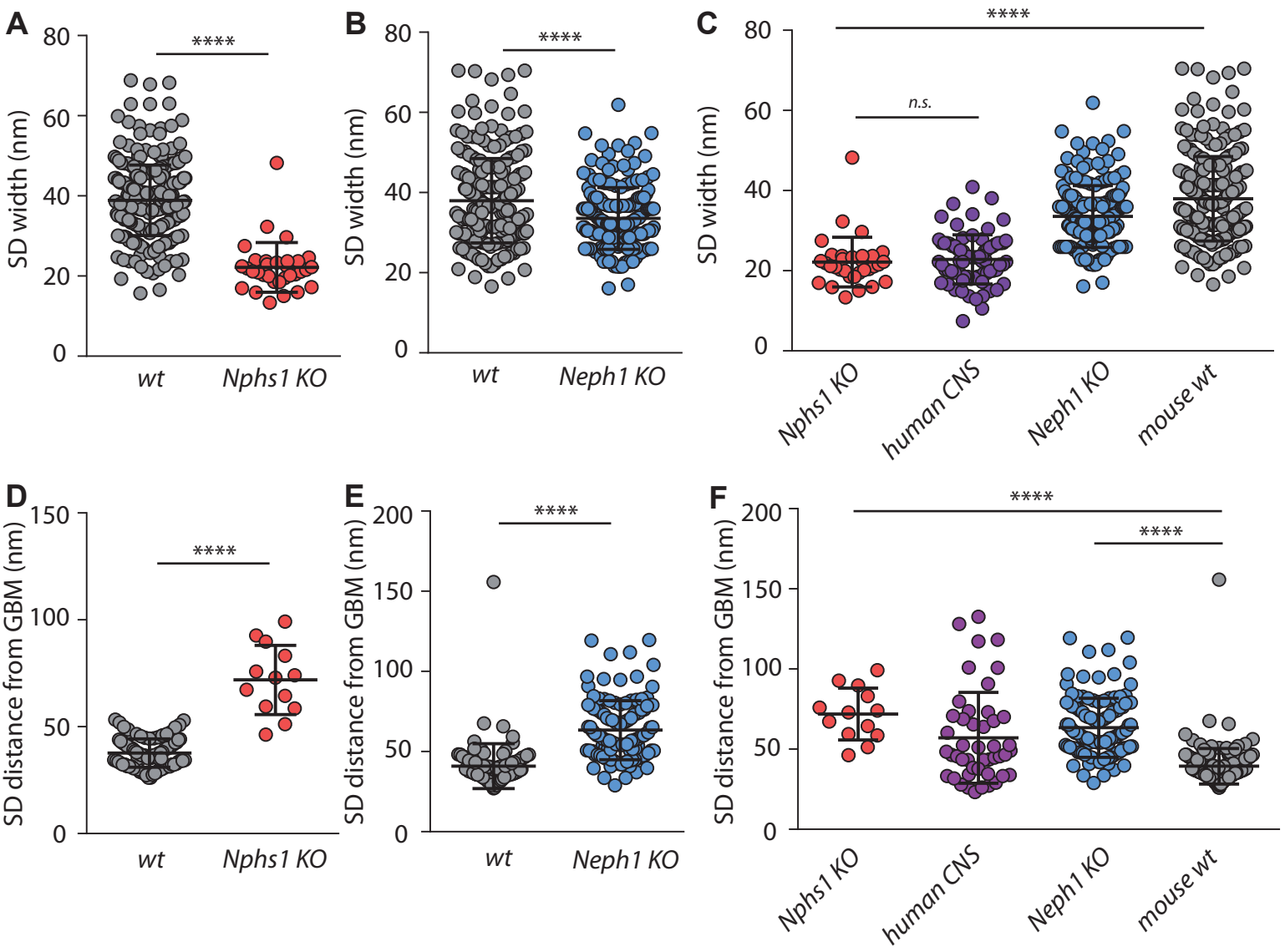

Supplemental Figure 4

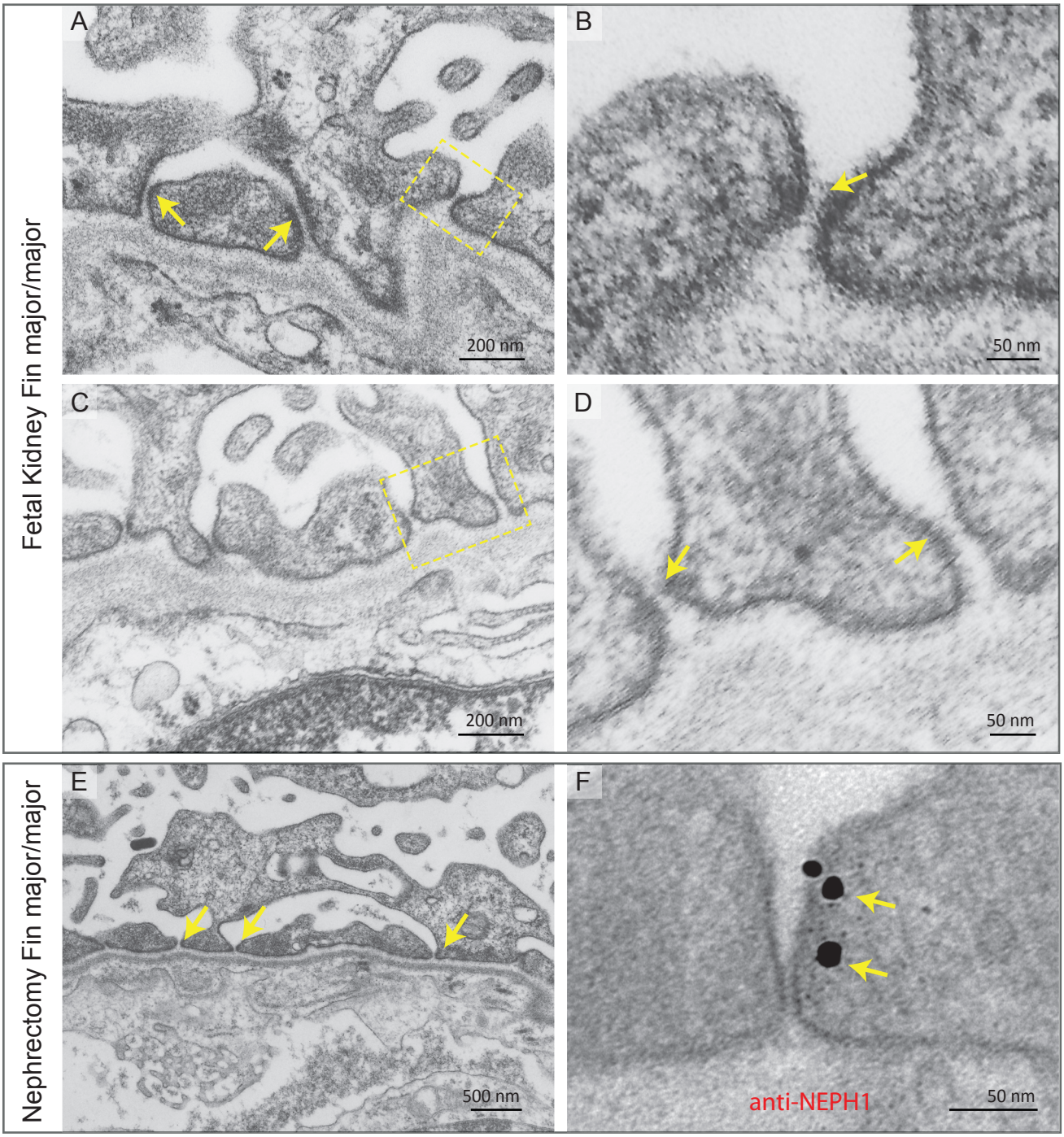

Supplemental Figure 5

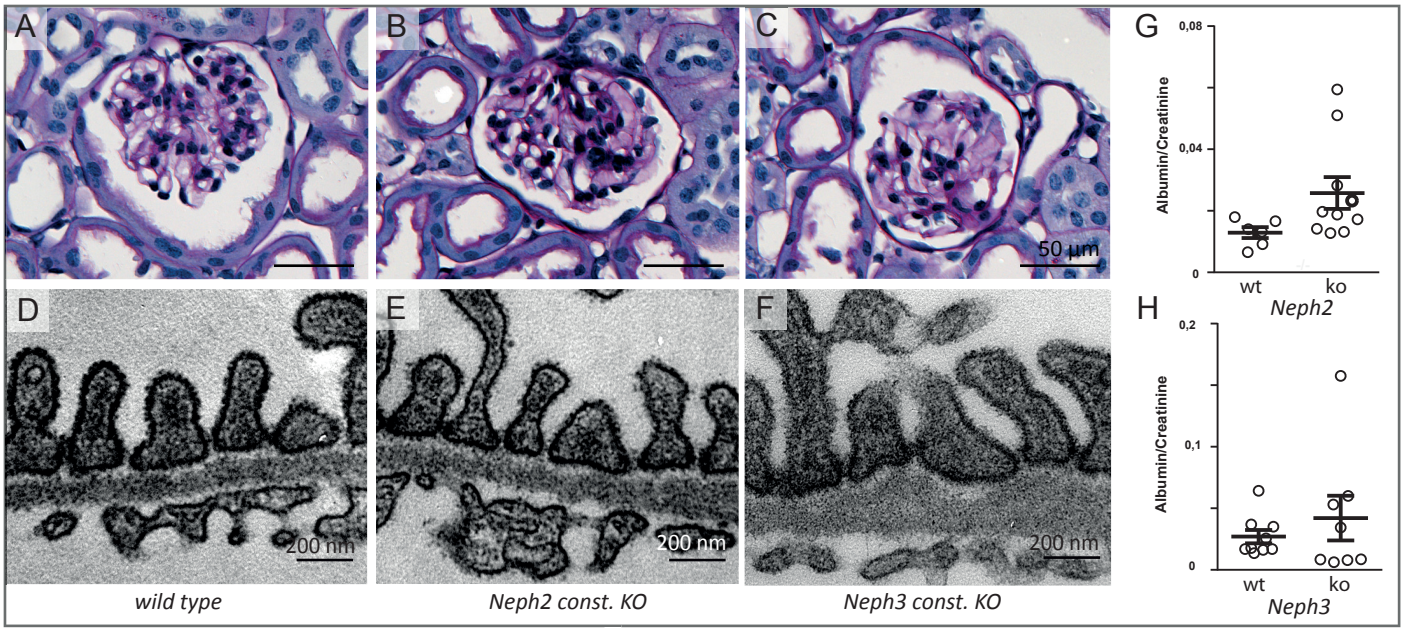

Supplemental Figure 6